

# Semi-Diurnal Tidal Periodicity Observed by an Ocean Bottom Seismometer Deployed at a Location Very Close to Seafloor Fumaroles in Wakamiko Caldera, Northeast of Sakurajima Volcano

Hiroshi YAKIWARA<sup>\*</sup>, Shuichiro HIRANO<sup>\*</sup>, Hiroki MIYAMACHI<sup>\*</sup>, Tetsuro TAKAYAMA<sup>\*\*</sup>,  
Tomoya YAMAZAKI<sup>\*\*\*</sup>, Takeshi TAMEGURI<sup>\*\*</sup> and Masato IGUCHI<sup>\*\*</sup>

(Received January 4, 2011; Accepted December 26, 2012)

An ocean bottom seismometer (OBS) recorded obvious semi-diurnal periodicity of the average velocity amplitudes of ground motions on the seafloor of Wakamiko Caldera (an active submarine volcano) northeast of Sakurajima Volcano in southwestern Kyushu, Japan. The ground motions were probably generated by the activity of the caldera's seafloor fumaroles, because we found bubbles ascending from those fumaroles just after deployment of the OBS. We compared changes in root-mean-square ground-velocity amplitudes in one-minute windows (RMSAs), tidal gravities (accelerations), and water levels during the observation period to obtain the characteristics of the periodicity. Those characteristics are summarized as follows: 1) We observed clear semi-diurnal periodicity of the RMSAs throughout September, 2007, though sometimes the periodicity was less obvious. 2) The timing of maxima RMSAs corresponded to maximum tidal gravities in the time domain. 3) The frequencies of four peaks seen in the power spectra of the changes in RMSAs were identical with those of the four major tidal components. 4) In detail, changes in RMSAs show saw-tooth shapes, and are irregular in periods of diurnal inequality. 5) Long-term or irregular changes in fumarole activity are possibly dominant in the period. The activity of hydrothermal fluids ascending from the deeper portion toward the seafloor fumaroles, which make up part of the circulation of a hydrothermal system, could be advanced as increasing upward tidal gravities (accelerations).

**Key words:** semi-diurnal periodicity, tidal gravity, ocean tide loading, seafloor fumaroles, Wakamiko Caldera

## 1. Introduction

Sakurajima Volcano is located in the northern part of Kagoshima Bay in southwest Japan. Most of Sakurajima Volcano is surrounded by the sea except its southeastern end (Fig. 1). Hypocenters of volcano-tectonic earthquakes that occurred around the volcano (Hidayati *et al.*, 2007) were located beneath the sea using data obtained by seismic stations on land. Seismic observations made by ocean bottom seismometers (OBSs) would provide more precise hypocenters and focal mechanisms for those earthquakes. In 2007 we performed seismic observation using two OBSs over two periods in order to obtain seismic data on the earthquakes that are generated beneath the bay. Although no volcano-tectonic earthquakes beneath the bay occurred during the monitoring periods, we found obvious semi-diurnal changes in root-mean square ground-velocity amplitudes in one-minute time windows observed by one

OBS installed on the seafloor of Wakamiko Caldera, northeast of Sakurajima Volcano (see Fig. 1). The clear, quasi-steady semi-diurnal periodicity agreed with the solid earth tide in the time domain throughout the observation period, which was over one month. Also, frequencies of four peaks derived from the power spectrum analysis for the changes in root mean squares are in good agreement with the frequencies of the four major tidal components.

Tides can influence the periodicity of submarine hydrothermal activity (Glasby and Kasahara, 2001). The semi-diurnal periodicity observed on the seafloor of Wakamiko Caldera, therefore, suggests that changes in solid earth tides and/or ocean tide loadings modulate submarine fumarole activity. Several researchers have investigated the periodicities of tectonic earthquakes or volcanic activity. Glasby and Kasahara (2001) reviewed the influence of tidal effects on the periodicity of tectonic earthquakes,

<sup>\*</sup>Nansei-Toko Observatory for Earthquakes and Volcanoes, Graduate School of Science and Engineering, Kagoshima University, 10861 Yoshino, Kagoshima 892-0871, Japan.

<sup>\*\*</sup>Sakurajima Volcano Research Center, Disaster Prevention Research Institute, Kyoto University, 1722-19 Sakurajima-Yokoyama, Kagoshima 891-1419, Japan.

<sup>\*\*\*</sup>Disaster Prevention Research Institute, Kyoto University, Gokasyo, Uji 611-0011, Japan.

Corresponding author: Hiroshi Yakiwara  
e-mail: yakiwara@sci.kagoshima-u.ac.jp

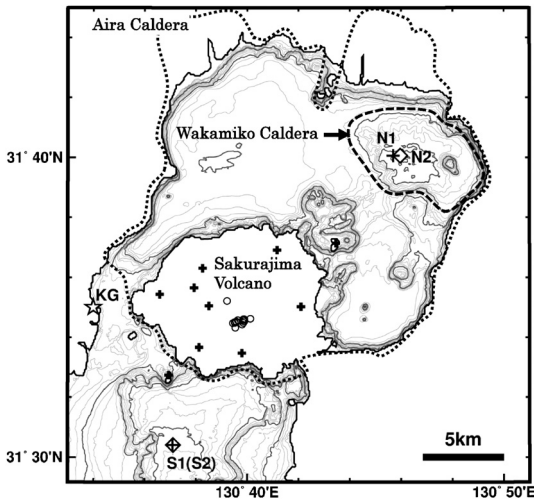


Fig. 1. Location of seismic stations. The locations of ocean bottom seismometers (OBSs) in the first and second observation periods are shown by crosses and diamonds, respectively. A star indicates the position of the Kagoshima Tidal Gauge. Thin and thick gray lines are the isobaths every 10 m and 50 m, respectively. Dotted curves illustrate the rims of calderas. Circles show the epicenters of volcanic earthquakes that occurred in the observation periods.

volcanic earthquakes, and submarine hydrothermal activity. Excluding tectonic earthquakes and non-volcanic deep tremors, several case studies of periodicity in volcanic or submarine hydrothermal activity were summarized in their review. Nasu *et al.* (1931) compared changes in water levels and the hourly numbers of earthquakes in and around the east Izu Peninsula for 6 days in 1930. They pointed out that times of low water corresponded with high earthquake frequency, and concluded that withdrawals of oceanic tide loading were the trigger actions that set in motions the hourly numbers of earthquakes. Rinehart (1972) investigated changes in the intervals between ejections of three geysers in the United States for about 6 months in 1967, and showed that short-term tidal forces and small earthquakes influenced periodic fluctuations in the intervals. Kasahara (1984) deployed an OBS at 3.5 days after the beginning of the eruptions of Miyakejima Volcano in 1983. They observed that the hourly numbers of earthquakes observed by the OBS increased at low-tide levels in the first stage of the observation period and high- and low-tide levels in the last stage.

Excepting Rinehart (1972), these case studies have compared only hourly numbers of events and tidal changes. However, Nishizawa *et al.* (1995) used an ocean bottom seismometer with a hydrophone (OBSh) at the Trans-Atlantic Geotraverse (TAG) hydrothermal field on the

Mid-Atlantic Ridge to record many pulse-shaped signals with periods of more than one minute. The seismometer recorded no ground motions corresponding to the signals. They also compared the average amplitudes of the hydrophone outputs and theoretical water levels (ocean tides) visually in the time domain over a period of one week and concluded that the averages showed obvious increases at low-water levels. Similar pulse-shaped events have also been detected in the South Mariana Trough (Sato *et al.*, 1995) and Middle Okinawa Trough (Kasahara *et al.*, 1995). In both these cases, the events were recorded only on the hydrophone channel, similar to Nishizawa *et al.* (1995). Sato *et al.* (1995) demonstrated that period of high activity corresponded to high-water levels over a period of eight days. Kasahara *et al.* (1995) compared event activity with solid earth and ocean tides for five days. Larger amplitude activity was observed just before earth tide minima, with some exceptions. The coincidence among the solid earth and ocean tides and the activity observed at the Okinawa and South Mariana troughs, however, were less obvious than that seen at the TAG.

After these periodicity studies, two studies showed the comparison between volcano activity and changes in tidal gravities (accelerations) in the frequency domain. Neuberg (2000) performed spectrum analysis and found that the periodicities of seismic noises observed at volcanoes (Ruapehu, Merapi and Batur volcanoes) had diurnal and semi-diurnal frequency peaks. The report also compared the observed peaks and the theoretical tidal gravities in the frequency domain, and concluded that the observed frequency peaks were distinguishable from the most prominent frequency components of tidal gravities, and that the periodicity was not caused by tidal gravities. In the figures of Neuberg (2000), we cannot recognize a correspondence between changes in volcanic activity and the theoretical tide gravities in the time domain. As candidates for the origin of the periodicity, Neuberg (2000) proposed other natural sources (temperature-induced stress fields, heavy rain, atmospheric pressure, and melting glaciers). Following Neuberg (2000), however, Hagerty and Sherburn (2002) rejected the periodicity observed at Ruapehu volcano as being a natural phenomenon. On the other hand, Custodio *et al.* (2003) presented an analysis of tidal periodicity of seismic noise and volcanic tremor observed at Fogo Volcano, Cape Verde. The seismic periodicity was strong enough to be detected by simple visual inspection of a long record of the raw signal (Custodio *et al.*, 2003). The most dominant spectrum peak, at 1.93 cycles per day, was obviously analyzed. A comparison of the seismic spectrum and the theoretical tidal gravities showed that the spectrum peak, with 1.93 cycles per day, agreed well with the most prominent component in the tidal gravities caused by the Moon. Unfortunately, the seismic signals were not compared to changes in tidal gravities in the time domain in the study.

To our knowledge, there is very little published literature that draws a parallel between signal amplitudes of volcanic or hydrothermal activities and changes in tides in the time domain. Most previous studies have been focused on either time sequences for numbers of earthquakes or spectrum peaks. Also, there are no reported periodicities of hydrothermal activity on shallow seafloors because observations using OBSs targeting seafloor hydrothermal activities have been carried out only in the deep-sea bottoms of troughs or mid-ocean ridges. This study presents a clear and steady semi-diurnal periodicity in time and frequency domain observed very close to the shallow-seafloor hydrothermal fumaroles of Wakamiko Caldera and discusses the cause of the periodicity, comparing the observed periodicity, changes in tide levels and solid earth tides.

## 2. Wakamiko caldera

Wakamiko Caldera (Kuwashiro, 1964; Shimomura, 1960) is a submarine caldera having a WNW-ESW elongated-ellipsoidal depression. It is located in the northeastern quarter of Aira Caldera (Matumoto, 1943). Wakamiko Caldera (6.5 km  $\times$  5 km) has flat bottom 200 m under the sea surface (Aramaki, 1984). Aira Caldera caused a huge eruption about 29,000 yrs B.P. (Aramaki, 1984; Nagaoka, 1988; Okuno, 2002). The eruption produced the Osumi pumice fall, the Tsuyama pyroclastic flow, and the Ito pyroclastic flow (Aramaki, 1984; Nagaoka, 1988). The total volume of its products has been estimated at about 150 km<sup>3</sup> (Machida, 2003). The vent of the largest eruption has been estimated to lie in the Wakamiko Caldera, based on the distribution of the dense breccia that erupted at an initial stage of the Ito pyroclastic flow (Nagaoka, 1988).

Fishermen have seen bubbles just below the sea surface in several areas in the extent of the caldera for many years. The bubbling phenomenon, called "Tagiri" by the local residents, provides visual evidence that volcanic activity of the caldera is still active. Chujo and Murakami (1976) conducted the first oceanographic survey of the area with a sub-bottom profiler in 1975. They found sea bottom fumaroles located in several areas on the submarine caldera floor. The profiler illustrated that the fumaroles generated many bubbles at the sea bottom, and the bubbles floated to the sea surface. Additionally, Osaka *et al.* (1992) investigated the submarine fumaroles in 1976, 1977, 1991 and 1992 using a submersible. They found over 30 areas with active fumaroles and collected samples of the volcanic gasses they emitted. They also measured temperatures just above the hydrothermal vents. The maximum temperature was 215° C. Yamanaka *et al.* (2001) did a geochemical study of Wakamiko Caldera's seafloor hydrothermal system. They investigated the fumaroles in 1998, 1999, and 2001 with a submersible to sample the shimmering fluids and bottom water around the fumaroles. Based on chemical analysis, their results suggest that hydrothermal circulation

occurs at the seafloor. Ishibashi *et al.* (2008) collected sediment and pore fluid samples from the seafloor with a submersible in 2003 and 2005 for geochemical analysis. They estimated the temperature of the geothermal reservoir to be 205° C using a silica geothermometer.

Hidayati *et al.* (2007) investigated the hypocenters and focal mechanisms of the volcano-tectonic earthquake activity of Sakurajima Volcano. They proposed a model that described the plumbing system of the magma beneath Aira Caldera and Sakurajima Volcano based on the regional stress field inferred from focal mechanism solutions and geodetic pressure sources obtained by GPS observation (Kriswati and Iguchi, 2003) and first-order leveling surveys (Eto *et al.*, 1998). A major magma reservoir related to the activity of the volcano probably exists between Sakurajima Volcano and Wakamiko Caldera at a depth of about 10 km. Because no other clear pressure source beneath the caldera was identified by the series of leveling surveys (*e.g.* Eto *et al.*, 1998), this reservoir may supply magma and volatiles to Sakurajima Volcano and seafloor fumaroles existing at Wakamiko Caldera.

## 3. OBS observation

In 2007 two pop-up type OBSs were used to conduct seismic observations during two monitoring periods. The OBS is composed of a three-component 4.5 Hz geophone (Mark Products, L28-BL) mounted on a gimbal, a data logger (Katsujima, KDR-224K) equipped with a high-accuracy timing module, and alkaline batteries in a glass sphere. The bearings of each horizontal component were unknown. The sampling rate was 64 Hz and the amplification factor for all channels of the recorder with 16-bit A/D converters was 40 dB. The digitized data was recorded using digital audiotape. The OBS can record continuous data for about two months, limited by the length of the tape and the total capacity of alkaline batteries.

In the first period of the observation, from August 30 through October 11 (42 days), an OBS was deployed on the seafloor of Wakamiko Caldera (Fig. 1, N1). Another OBS was installed on the sea bottom in the south of the volcano (Fig. 1, S1). As soon as the OBS at N1 was thrown overboard, we confirmed visually bubbles ascending toward the sea surface below the release point. We, therefore, expected that the OBS at station N1 was deployed very close to seafloor fumaroles. In the second period, from October 26 through December 14 (48 days), we deployed the same OBS units again. As the OBS deployed at N1 had recorded ground motions of which the amplitudes were relatively large compared to those recorded at S1, station N2 was designed to be situated about 430 m east of station N1 (Fig. 1, N2). The OBS at station S2, on the other hand, was planned to be deployed as close as possible to the coordinates of S1 using the real-time position of the vessels and navigation tools. The operation was able to place the OBS deployed at S2 only 13.8 m

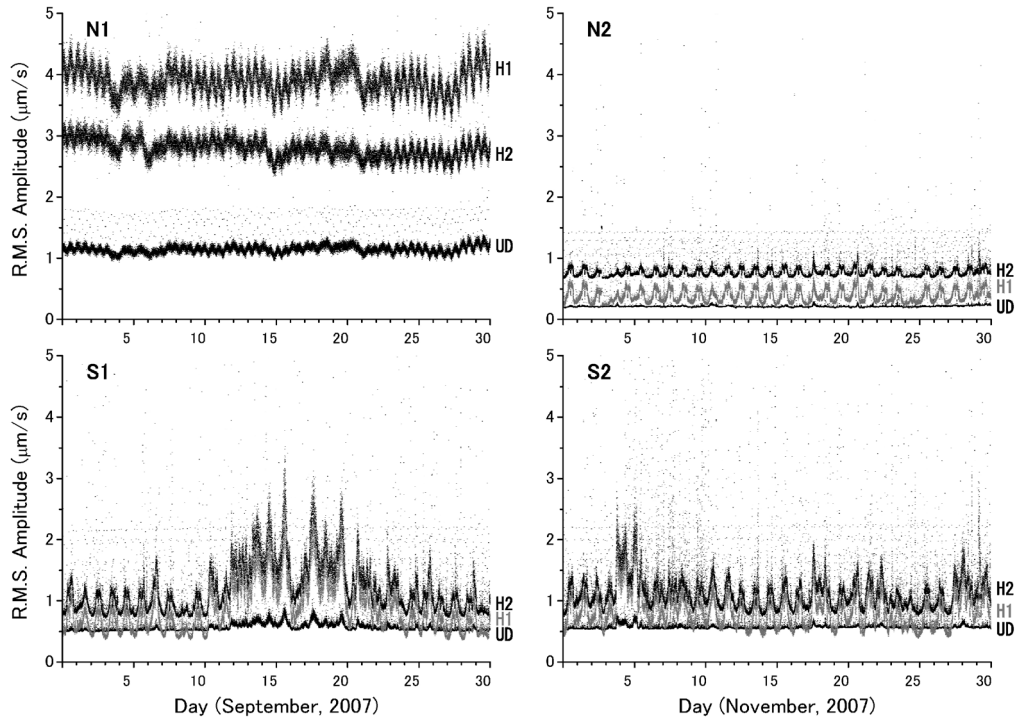


Fig. 2. Time changes, for 30 days (one month), in the unfiltered root-mean squares of velocity amplitudes in one minute windows (RMSAs) for each component for the ocean-bottom seismometers; UD is the vertical component; H1 and H2 are horizontal components.

horizontally from the position of S1.

The internal clock of each OBS was calibrated just before deployment and after retrieval by comparing it to a GPS clock. The internal clock data were adjusted using the two time-calibration data points, assuming that the drift rate was constant during the period of observation. After the time calibrations were performed, we found that the internal clock of the OBS deployed at N1 and N2 fluctuated several times within a few seconds, possibly being stepwise drifts. Although we could not use the data recorded at N1 and N2 for hypocenter determinations of earthquakes, the slight fluctuation did not affect the results of the present study.

The deployments and retrievals of the OBSs were carried out by a working vessel of 15 gross tons. Because the vessel had no navigation tool, a DGPS antenna and receiver system (SOKKIA, R80D) and the laptop computer that the electronic navigation charts (ENCs) issued by the Japan Coast Guard were installed, were used to guide the vessel to the objective survey positions. The computer's navigation software (PC Studio Alpha, AlphaMap, Lite edition) displays the real time position of the vessel, ENCs, bathymetric maps, and the objective approach points simultaneously. Heading data issued by a GPS unit (Germin, eTrex series, Vista) were also used to navigate

incorporating in the software.

The coordinates and depths of each OBS station were determined as follows. The vessel was navigated to four points. One was the OBS release position, and the other three form a triangle surrounding that point. The horizontal distances between the centroid and each vertex were nearly equal to the depth of the OBS estimated using the bathymetric map. At each point, we measured direct distances with acoustic signals between the vessel and the deployed OBS several times. The vessel coordinates were logged using the DGPS. The distance data and vessel coordinates at the moment of the each measurement were inverted to calculate the coordinate and depth of the OBS.

#### 4. Observed periodicity of ground motion velocity amplitudes

##### 4-1 Changes in root-mean-squares amplitude

Root-mean-squares amplitudes in one-minute time windows (herein termed RMSAs) were calculated from the continuous ground velocity data recorded by the OBSs in order to compare them. Not only the continuous ground velocity data but also the RMSAs in this study were not filtered. Fig. 2 shows changes in RMSAs on three (one vertical and two horizontal) components at each station for two 30-day periods in September and November, 2007. The vertical and both horizontal RMSAs observed at N1

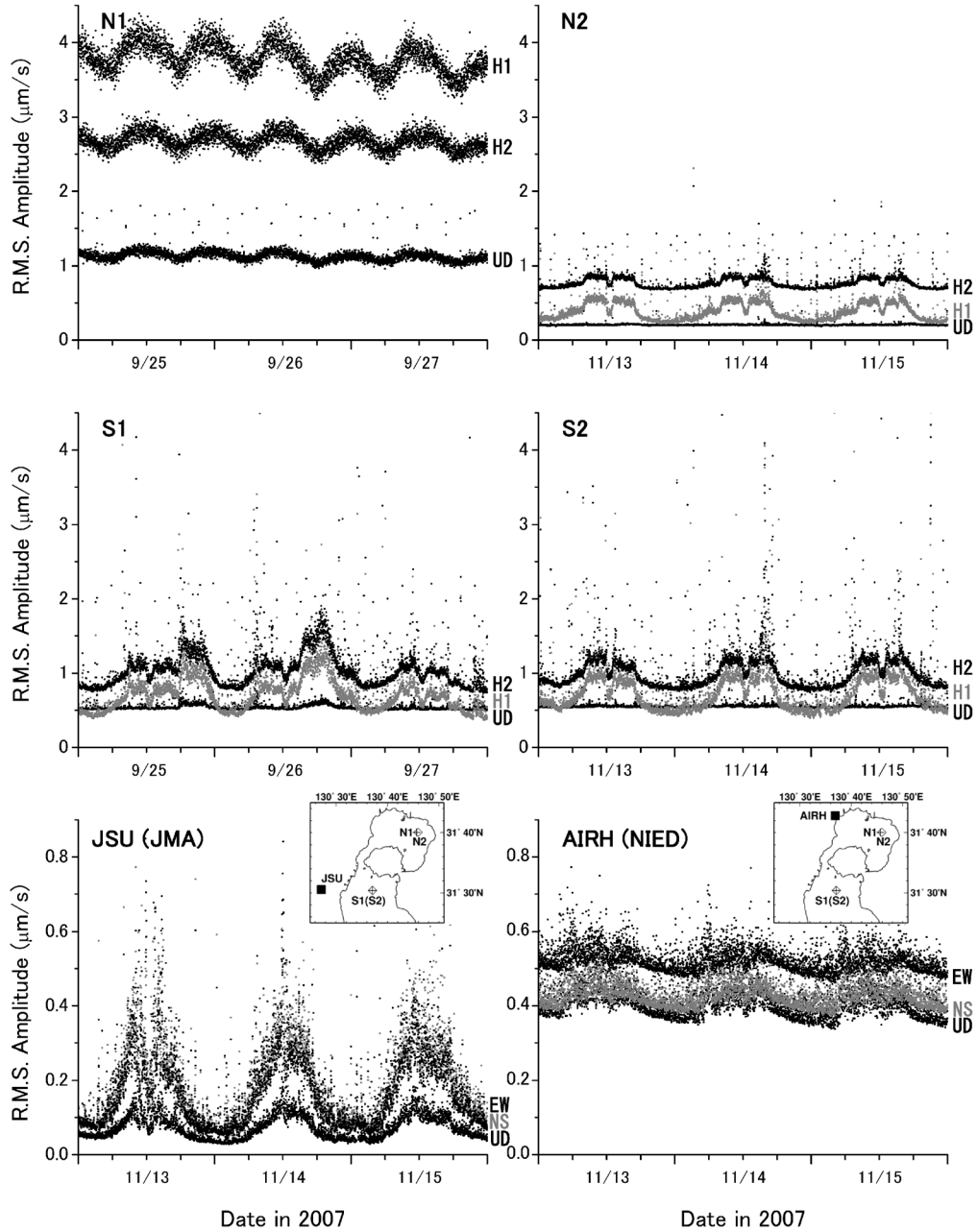


Fig. 3. RMSA changes for 3 days. UD, H1, and H2 are the same as in Fig. 2. The RMSA changes observed simultaneously at the two seismic stations (JSU and AIRH) on land are also shown. The locations of the stations are plotted in the maps.

were remarkably larger than those at the other stations. Although station N2 was only about 430 m eastward from station N1, the RMSAs at N1 were several times larger than those at N2. At deployment, as soon as we released the OBS into the sea above station N1, we saw bubbles below the sea surface, so we presumed that the OBS on the

sea bottom at N1 was deployed very close to highly active seafloor fumaroles. On the contrary, it is possible that no seafloor fumaroles existed near station N2, because we saw no bubbles on the sea surface above N2 at deployment and retrieval of the OBS. As mentioned above, the OBS deployed at N1 probably recorded ground motions related

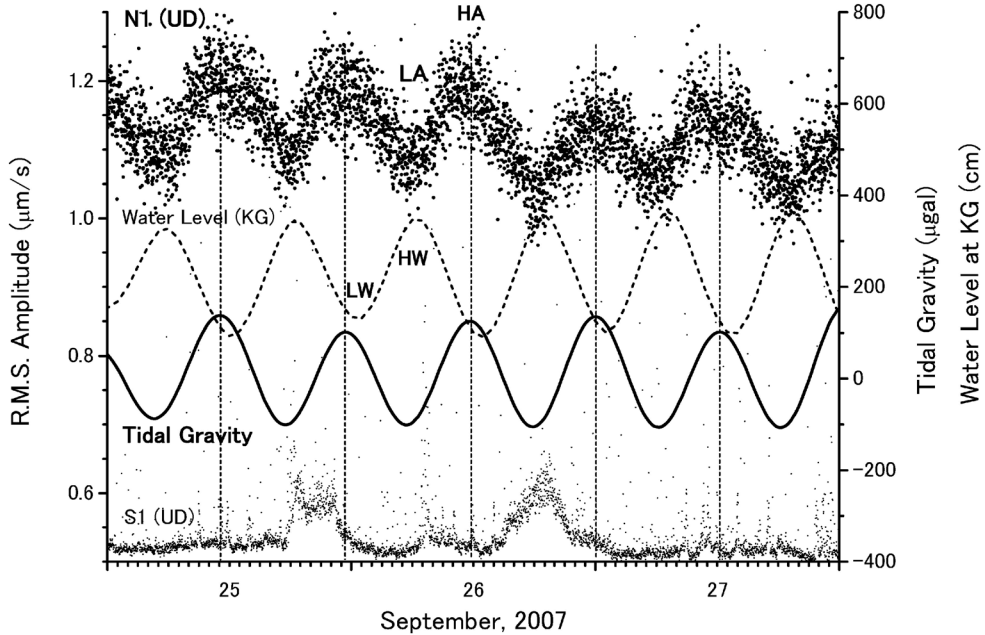


Fig. 4. Comparison of time changes in RMSAs, water levels, and tidal gravities for three days. The top and bottom plots (scale at left) show the RMSA changes over time at N1 and S1, respectively. The second (dotted) curve (scale at right) is the change over time of water levels observed at KG. The third (thick) curve (scale at right) shows changes in theoretical tidal gravities (accelerations). Examples of times where maximum and minimum RMSAs occurred at N1 are labeled HA and LA. HW and LW show the timing of the maximum and minimum water levels, respectively. Vertical dotted lines correspond to the time of maximum RMSAs at N1.

to seafloor fumarole activity.

#### 4-2 Characteristics of RMSA changes

In Fig. 2 the RMSAs on the horizontal components of each station are recognized as mostly quasi-regular. Noticeable RMSAs increases at S1 from September 11 to 20 were possibly excited by two strong typhoons that passed near Kyushu Island. Additionally, the OBSs at S1 and S2 were set under well-used navigation routes and near anchorage positions in Kagoshima Harbor, so it suffered from vessel noises. Therefore, episodic, irregular increases are seen in the RMSAs at S1 and S2. On the other hand, the characteristics of the RMSAs at N1 are different from those of the other stations as described below.

Fig. 3 shows the changes in RMSAs on each component for three consecutive days (September 25 through 27, 2007 at N1 and S1 and November 13 through 15, 2007 at N2 and S2). The semi-diurnal changes in the RMSAs at N1 are clearly observable and are independent of the days and nights. The RMSAs have maxima at about noon and midnight, and minima in the morning and evening over the three days. Because the OBS at N1 was probably deployed very close to seafloor fumaroles, the semi-diurnal periodicity observed at N1 suggested that the amplitudes of ground motions generated by the high activity of the sea-

floor fumaroles correlated with periodic phenomenon such as ocean tide loadings. On the other hand, the changes in RMSAs on the horizontal components at the other stations (N2, S1 and S2) illustrate “mountain-shaped” diurnal changes; increases and decreases during the daytime and nighttime, respectively. Also, a sudden decrease in the RMSAs occurred just after noon for about one hour. The characteristics of the horizontal RMSAs at N2, S1 and S2 were probably generated by human activities around the bay. The mountain-shaped changes are not seen in vertical RMSAs but are prominent only in horizontal RMSAs (Fig. 3, N2, S1 and S2), possibly because artificial noises from land are incident from the almost horizontal direction. On the other hand, the changes in the RMSAs on vertical component of the ground motion observed at two permanent seismic stations on land (Fig. 3, JSU and AIRH) obviously draw mountain shape. On the contrary no mountain-shaped change is shown in N1’s RMSAs. The relatively large amplitudes of the ground motions observed at N1 probably hide the artificial noises.

#### 4-3 Comparisons between RMSAs and tidal phenomena

Fig. 4 compares the RMSAs on vertical components of ground velocity at N1 and S1 to changes in water levels

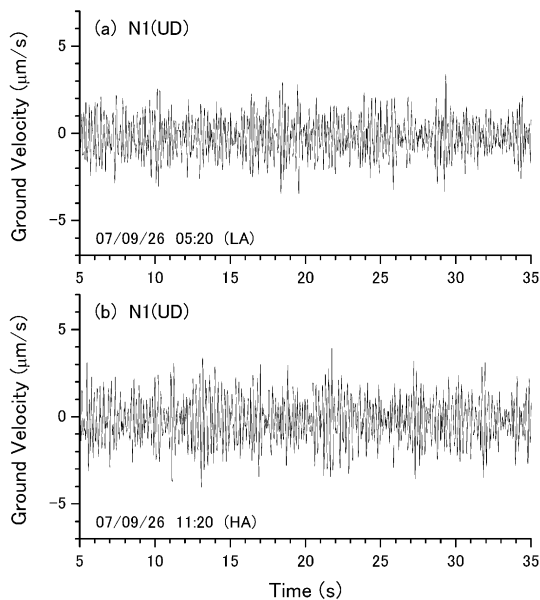


Fig. 5. Examples of the raw waveforms (ground velocity, vertical component) observed at the time of minimum and maximum RMSAs. The times of LA and HA are the same as in Fig. 4.

observed by the Japan Meteorological Agency's Kagoshima Tidal Gauge of (Fig. 1, KG) for three days from September 25 through 27, 2007. The maxima and minima of the RMSAs at N1 (Fig. 4, LA and HA) clearly preceded at the times of the low- and high-water (Fig. 4, LW and HW) by about one hour. The relation between the RMSAs and the water-level peaks observed at KG was not seen at S1. Aperiodic changes in the RMSAs at S1 did not correlate to the time sequence of the sea water level. Fig. 5 shows an example of the raw velocity waveforms (the vertical component of N1) observed at the times of LA and HA (Fig. 4). Visually, we can recognize that the amplitudes of the waveforms recorded at HA are slightly larger than those at LA.

The ocean tide loading hardly explains why the maxima and minima RMSAs precede at the times of the low- and high-water. Therefore, we used a source cord (Nakai, 1979) to calculate the forces of the solid earth tide to compare with the changes in RMSAs observed at N1. The program computes, given any position on the earth's surface and a time, the tidal gravity (vertical derivative of tidal potential) due to the relative astronomical positions of the Earth, Moon and Sun. Fig. 4 also draws a parallel between the RMSAs on the ground velocities observed at N1 and the tidal gravities in the time domain. The maxima and minima RMSAs at N1 are in sync well with maxima and minima tidal gravities over the three days. The vertical RMSAs observed at N1 increase as the tidal

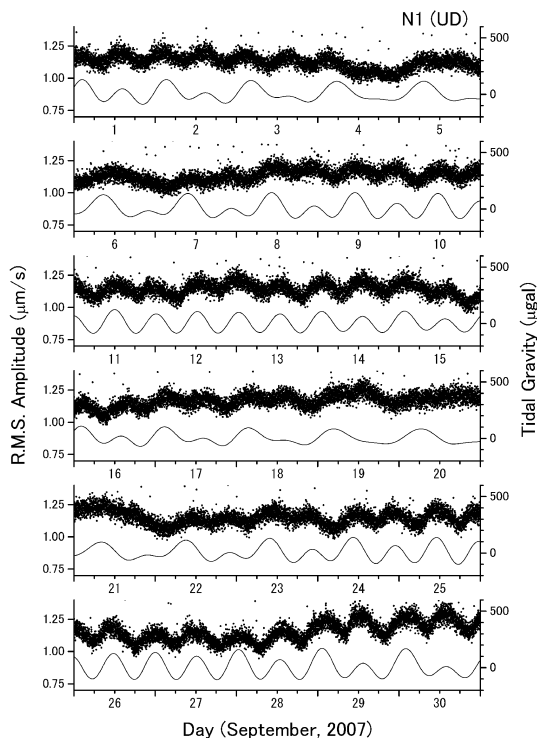


Fig. 6. Comparison between RMSA changes over time at N1 and theoretical tidal gravities (accelerations) for 30 days (September, 2007). Dots and curves are the RMSAs (scale at left) and the gravities (scale at right).

gravities become larger, and decrease as the tidal gravities are reduced. Visual inspection of Fig. 4 shows clearly that there is a strong positive correlation between changes in RMSAs at N1 and tidal gravities, even without spectrum analysis. Figure 6 compares changes in vertical RMSAs at N1 and tidal gravities over 30 days in September, 2007. With the exception of periods of diurnal inequality (i.e. from September 19 through 22), the correlation is obvious throughout the period. The obvious semi-diurnal periodicity observed at N1 is probably a quasi-steady phenomenon associated with the seafloor fumaroles. In addition, irregular components like the step-like changes in RMSAs at N1 may reflect changes in activity of the submarine fumaroles. The long-term changes in the RMSAs shown in periods of diurnal inequality may correlate with changes of seafloor fumarole activity.

In order to find the prominent frequencies of the periodicity, we analyzed power spectra using the changes in RMSAs at N1 over 30 days in the month. We then compare the frequencies and the major tidal components of harmonics. Fig. 7 shows the power spectra of the changes in RMSAs and theoretical tidal gravities. It is possible that four peaks corresponding to the four major tidal

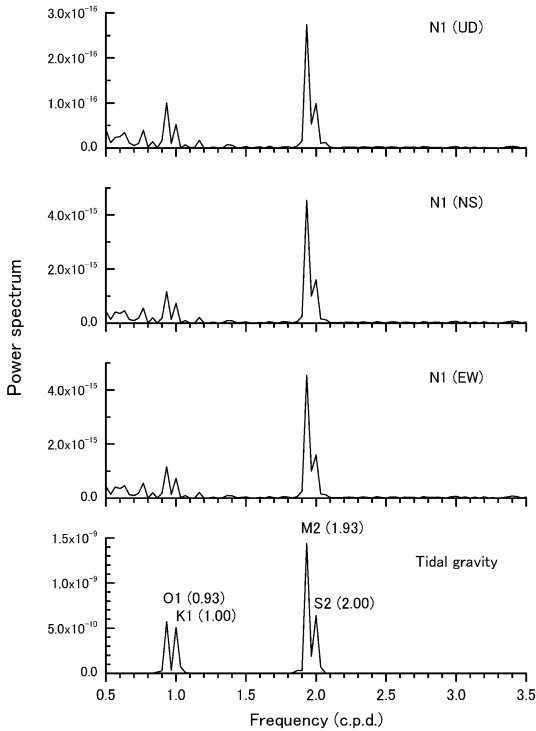


Fig. 7. Power spectra of the RMSAs at N1 very close to seafloor fumaroles using data on 30 days in September, 2007. Spectrum of the theoretical tidal gravities calculated by Nakai (1977) is also shown. The names and peak frequencies (cycles per day; c.p.d.) of the four major tidal components are written in the bottom spectrum.

components M2, S2, K1, and O1 are clearly seen. The frequency of the largest peak is identical with that of the M2 (1.93 c.p.d.) component. Another semi-diurnal peak (2.00 c.p.d.) can be recognized, and corresponds to the frequency of component S2. Two diurnal peaks are also obvious in the spectra and agree with components K1 (1.00 c.p.d.) and O1 (0.93 c.p.d.), respectively. Additionally, relative magnitudes on each peak of RMSAs also can be explained qualitatively by the relation of the four tidal components. As described above, a close relationship between the RMSAs at N1 and the tidal gravities is apparent. Therefore, we concluded that the changes in RMSAs at N1, which probably reflect ground motions related to seafloor fumaroles, had a strong correlation to tidal gravities in the time and frequency domain.

Strictly speaking, the changes in RMSAs at N1 do not precisely correspond to the tidal gravities, because the RMSAs at N1 in the period shown in Fig. 4 do not appear as a sine curve but are saw-toothed and slightly asymmetrical. The changes in the RMSAs seem to be slightly

steeper on the left of the vertex, and the absolute values of the gradients of increasing RMSAs are somewhat steeper than the decreasing ones. The RMSAs decrease slowly after the maxima. An opposite relation between changes in RMSAs and tidal gravities, however, were observed on September 28 and 29 (Fig. 6). In Fig. 6, the timing of several peaks of the tidal gravities is different from changes in the RMSAs. The relation between the RMSAs and tidal gravity may not be a linear, but a non-linear relation.

## 5. Discussion

We found semi-diurnal periodicity of the changes in RMSAs observed at the sea bottom very close to active shallow seafloor fumaroles in Wakamiko Caldera, although the periodicity was sometimes not so obvious. There are two important characteristics of the changes in RMSAs. The first is a one month long quasi-steady phenomena that correspond to tidal gravity in the time and frequency domain. The second is that the changes in RMSAs show saw-tooth shapes and are irregular in periods of diurnal inequality. To our knowledge, the quasi-steady month-long tidal-periodicity of amplitudes of ground motions has not been reported by previous studies. The semi-diurnal periodicity observed at the TAG (Nishizawa *et al.*, 1995) was not recorded by a seismometer but only a hydrophone. The present semi-diurnal periodicity, therefore, differs from the phenomena observed at the TAG. The time sequences in velocity amplitudes of ground motions observed at Fogo volcano (Custodio *et al.*, 2003) for 5.5 days were compared with tides not in the time domain but only in the frequency domain. Thus we cannot make a detailed comparison between the Fogo volcano's periodicity and the present one.

Most of the maxima RMSAs were observed around the times of maximum tidal gravities (accelerations). This relationship may indicate that the upward tidal forces drive the increased activity of the seafloor fumaroles. Also, the time lags between the RMSAs and tidal accelerations are quite small or nonexistent. These characteristics would suggest that the activity responds readily to variations in external forces. Ocean tide loadings may also affect changes in RMSAs. As described in the previous section, the slightly asymmetrical changes in the RMSAs suggest that the relation between the RMSAs and tidal gravities may be a non-linear relation. We should therefore investigate why the changes in RMSAs are not symmetrical but slightly asymmetrical. Because tidal loadings reach maxima about one hour late, the loadings may delay rises in the fumarole's activity. Also, delay of the minima tidal loading by about one hour may attenuate the decrease rate of the activity of the fumaroles in initial of the declining stage. Let us consider the tidal forces acting on the seafloor as a superposition of the tidal gravities and the ocean tide loadings. The loadings per unit area are equal to the hydro-

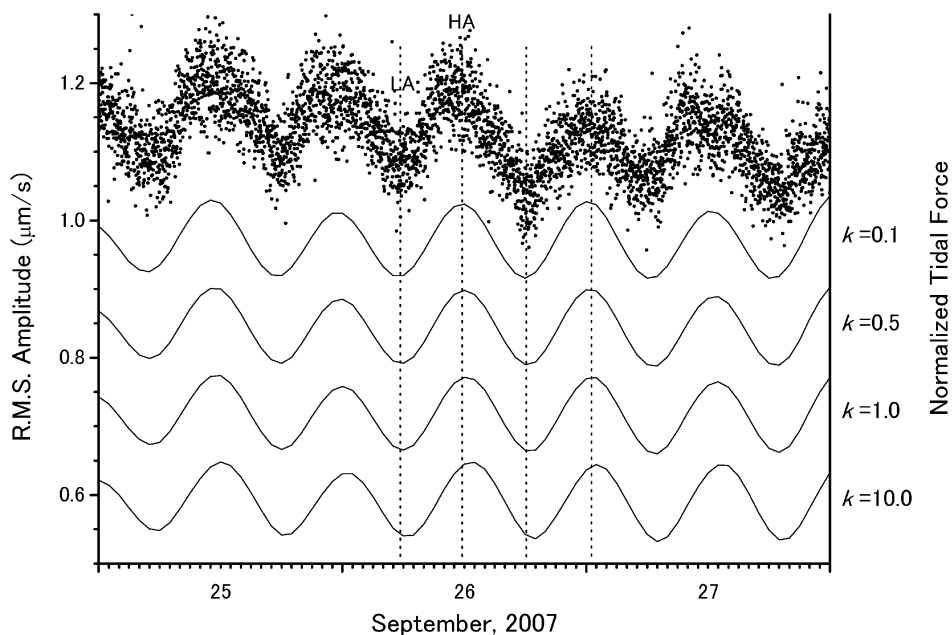


Fig. 8. Results of a simple simulation assuming a linear combination of tidal gravities (accelerations) and ocean tide loadings. The RMSAs at N1 are also shown by dots (scale, left). The constant of proportionality,  $k$ , corresponds to the relative weight of the ocean tide loadings. The thin curves are the normalized tidal forces calculated with four values of the constant. The constant increases with increasing relative weight.

static pressure, increasing in proportion to water depth. Assuming that the RMSAs respond linearly to the combination, and in proportion to the tidal accelerations (forces per unit bulk) and ocean tide loadings, a simple relation with no time lag, because of the response instance, is derived as

$$RMSA(t) = c0[a \cdot tg(t) - b \cdot wl(t)] \quad (1)$$

Here, the terms  $tg(t)$  and  $wl(t)$  are the time changes of the normalized tidal acceleration and water levels observed at KG (Fig. 1) using maximum values of those, and  $a$ ,  $b$  and  $c0$  are constants of proportionality. The second term in the square bracket of the right hand of Eq. (1),  $b \cdot wl(t)$ , relates to the ocean tide loadings. The negative sign of the term assumes that the activity of the fumaroles is repressed as the hydrostatic pressure increases. The coefficients express the strengths of the tidal accelerations and the loadings. Moreover, generalizing the relation in Eq. (1), we obtain the following simple model using coefficients  $c1$  and  $k$ .

$$RMSA(t) = c1[tg(t) - k \cdot wl(t)] \quad (2)$$

Here,  $c1 = c0 \cdot a$ , and  $k = b/a$ . Coefficient,  $k$ , shows the relative strength (weight) of the tide loadings to the accelerations; the weight of the loadings increases as the coefficient increases. We provide several values of the coefficient,  $k$ , to compare with the changes in RMSAs.

Fig. 8 shows the relative changes in RMSAs calculated using four values of  $k$ . Normalized curves are shown in the figure. If the coefficient is large, the contribution of the ocean tide loadings increases, and the peaks of the calculated RMSAs are later than those observed. It suggests that the changes in RMSA are mainly controlled by tidal acceleration of solid earth tides. As a result of the simple model, no values of  $k$  do the saw-tooth shapes of the RMSAs appear. Thus, the superimposition of tidal gravities and ocean tide loadings can hardly explain the slightly asymmetrical changes in RMSAs. Interestingly, the left side of the RMSAs is relatively steep with more gradual decreases during the decreasing tidal stage (i.e. on September 13, Fig. 6). On the contrary, the right side is relatively steep during increasing tidal stages (i.e. from September 28 through 29, Fig. 6). Long-term changes in seafloor activity may cause asymmetric changes in RMSAs. Ishibashi *et al.* (2008) suggested that area of hydrothermal circulation of Wakamiko Caldera must be horizontally as large as 5 km on the basis of an investigation of the isotropic composition of the hydrothermal component of the caldera. The hydrothermal system is thought to be driven by a magmatic heat source beneath the caldera (Ishibashi *et al.*, 2008). The active fumaroles on the seafloor play the role of discharging fluids in the hydrothermal circulation around Wakamiko Caldera. The hydrothermal fluids ascending from the deeper portion

toward the seafloor fumaroles may advance with increasing upward tidal forces because of the permeable seabottom sediments. This idea is supported by the fact that the semi-diurnal periodicity disappears in periods of diurnal inequality, while activity variations are dominant in the RMSAs changes. Inertia of the hydrothermal fluids ascending may cause the slightly asymmetrical changes in RMSAs observed at N1.

## 6. Conclusion

Using an ocean bottom seismometer, we observed obvious quasi-steady semi-diurnal periodicity of the average ground motion at the sea bottom very close to seafloor fumaroles in Wakamiko Caldera, an active submarine volcano, located in the northeastern quarter of Aira Caldera. We compared changes in root-mean-square ground-velocity amplitudes in one-minute windows (RMSAs) with tidal gravities (accelerations) and water levels to obtain the characteristics of the periodicity as follows.

1) The semi-diurnal periodicity in RMSAs observed at Wakamiko Caldera was probably caused by fumarole activity.

2) The periodicity was clearly observed throughout September, 2007, though sometimes it was less obvious. The timing of maxima RMSAs corresponded to the timing of maxima tidal gravity in the time domain. Frequencies of the prominent four peaks seen in the power spectra are identical to those of the four major tidal components (M2, S2, K1, and O1).

3) The changes in RMSAs show saw-tooth shapes, and are irregular in periods of diurnal inequality. Long-term or irregular changes of activity of the fumaroles are possibly dominant in the period.

We proposed a simple model that relates the change in tidal force, as represented by a superimposition of tidal gravities and ocean tide loading effects to changes in RMSAs, without time lag, to reproduce the characteristic of the observed saw-tooth changes in RMSAs. Although the model cannot explain the saw-tooth changes, it suggests that changes in RMSAs are mainly controlled by tidal acceleration of solid earth tides. The activity of hydrothermal fluids ascending from the deeper portion toward the seafloor fumaroles can be advanced as increasing upward tidal forces.

## Acknowledgements

We thank the captain of the working vessel, Mr. K. Kawabata, for skillful operating the vessel on the voyages to deploy and retrieve the OBSs. We are grateful to the secretary, Mr. S. Koyanagi, of the East Sakurajima fishermen's cooperative association and the Japan Fisheries cooperative of Kagoshima Prefecture for accepting our operation. We acknowledge Prof. T. Kobayashi of Kagoshima University for his useful suggestion about the eruption histories of Aira and Wakamiko Caldera. We

express our sincere thanks to Prof. H. Shimizu of Kyushu University for special suggesting the relation among the observed periodicity, the tidal gravities, and the ocean tide loadings. The suggestions of two anonymous referees also led to significant improvements in this study. We acknowledge the Japan Meteorological Agency (JMA) for use of the data set of water levels observed at Kagoshima Tidal Gauge, downloaded from the JMA homepage. We used the continuous waveform data opened to the public by National Research Institute for Earth Science and Disaster Prevention (NIED) and JMA. We thank the agencies for their technical assistances.

## References

- Aramaki, S. (1984) Formation of the Aira caldera, southern Kyushu, ~22,000 years ago. *J. Geophys. Res.*, **89**, 8485–8501.
- Chujo, J. and Murakami, F. (1976) The geophysical preliminary surveys of Kagoshima Bay. *Bull. Geol. Surv. Jpn.*, **12**, 807–826 (in Japanese).
- Custodio, S. I. S., Fonseca, J. F. B. D., d'Oreye, N. F., Faria, B. V. E. and Bandomo, Z. (2003) Tidal modulation of seismic noise and volcanic tremor. *Geophys. Res. Lett.*, **30**, 1816, doi: 10.1029/2003GL016991.
- Eto, T., Takayama, T., Yamamoto, K., Hendrasto, M., Miki, D., Sonoda, T., Kimata, F., Miyajima, R., Matsushima, T., Uchida, K., Yakiwara, H. and Kobayashi, K. (1998) On the result of leveling surveys around Sakurajima volcano during December 1991 to October 1996. In *9th Joint observation of Sakurajima volcano* (Ishihara, K. ed). Sakurajima Volcano Research Center, Kagoshima, 15–29 (in Japanese).
- Glasy, G. P. and Kasahara, J. (2001) Influence of tidal effects on the periodicity of earthquake activity in diverse geological settings with particular emphasis on submarine hydrothermal systems. *Earth-Sci. Rev.*, **52**, 261–297.
- Hagerty, M. and Sherburn, S. (2002) Comment on 'External modulation of volcanic activity' by J. Neuberg. *Geophys. J. Int.*, **148**, 692–694.
- Hidayati, S., Ishihara, K. and Iguchi, M. (2007) Volcano-tectonic earthquakes during the stage of magma accumulation at the Aira caldera, southern Kyushu, Japan. *Bull. Volcanol. Soc. Japan*, **52**, 289–309.
- Ishibashi, J., Nakaseama, M., Seguchi, M., Yamashita, T., Doi, S., Sakamoto, T., Shimada, K., Shimada, N., Noguchi, T., Oomori, T., Kusakabe, M. and Yamanaka, T. (2008) Marine shallow-water hydrothermal activity and mineralization at the Wakamiko crater in Kagoshima bay, south Kyushu, Japan. *J. Volcanol. Geotherm. Res.*, **173**, 84–98.
- Kasahara, J. (1984) Miyakejima eruption and ocean bottom observation-seismic activity, tidal change and spiky phases. *Monthly Chikyu*, **6**, 749–754 (in Japanese).
- Kasahara, J., Saito, T. and Koresawa, S. (1995) Evidence for periodic hydrothermal activity at the hydrothermal vent in the Iheya knolls, in the Okinawa trough, Japan, measured by an OBS/H with the assistance of the submersible

- “Shinkai 2000”. *JAMSTEC Deep-sea Res.*, **11**, 167–188.
- Kriswati, E. and Iguchi, M. (2003) Inflation of the Aira caldera prior to the 1999 eruptive activity at Sakurajima Volcano detected by GPS network in South Kyushu. *Ann. Disast. Prev. Inst., Kyoto Univ.*, **46**, 817–826.
- Kuwashiro, I. (1964) On the proto-caldera, the case of the Aira caldera. *J. Geogr.*, **73**, 114–120 (in Japanese).
- Machida, H. (2003) **Atlas of Tephra in and around Japan**, revised edition. Univ. Tokyo Press, 337 pp (in Japanese).
- Matumoto, T. (1943) The four gigantic caldera volcanoes of Kyushu. *Jap. J. Geol. Geogr.*, **19**, Special number, 1–58.
- Nagaoka, S. (1988) The late quaternary tephra layers from the caldera volcanoes in and around Kagoshima Bay, southern Kyushu, Japan. *Geogr. Rep. Tokyo Metro. Univ.*, **23**, 49–122.
- Nakai, S. (1979) A subroutine program for computing the tidal forces for the practical use. *Proc. Inter Latitude Obs. Mizusawa*, **18**, 124–135 (in Japanese with English abstract).
- Nasu, P., Kishinouye, F. and Kodaira, T. (1931) Recent seismic activities in the Idu peninsula (Part I). *Bull. Earthq. Res. Inst.*, **9**, 22–35.
- Neuberg, J. (2000) External modulation of volcanic activity. *Geophys. J. Int.*, **142**, 232–240.
- Nishizawa, A., Sato, T., Kasahara, J. and Fujioka, K. (1995) Tide related activity observed by OBSH on the TAG hydrothermal mound. *JAMSTEC Deep-sea Res.*, **11**, 125–135 (in Japanese with English abstract).
- Okuno, M. (2002) Chronology of tephra layers in southern Kyushu, for the last 30,000 years. *Quarter. Res.*, **41**, 225–236 (in Japanese).
- Ossaka, J., Hirabayashi, J., Nogami, K., Kurosaki, M. and Hashimoto, J. (1992) Variation of chemical composition of volcanic gases from the northern part of Kagoshima bay. *Proc. JAMSTEC Symp. Deep Sea Res.*, 75–77 (in Japanese with English abstract).
- Rinehart, J. S. (1972) Fluctuations in geyser activity caused by variations in earth tidal forces, barometric pressure, and tectonic stresses. *J. Geophys. Res.*, **77**, 342–350.
- Sato, T., Kasahara, J. and Fujioka, K. (1995) Observation of pressure change associated with hydrothermal upwelling at a seamount in the south Mariana Trough using an ocean bottom seismometer. *Geophys. Res. Lett.*, **22**, 1325–1328.
- Shimomura, H. (1960) Topographic division for Aira depression caldera. *Hiroshima Univ. Stu., Litera. Dep.*, **18**, 308–331 (in Japanese).
- Yamanaka, T., Ishibashi, J., Nakano, A., Ueki, Y. and Hashimoto, J. (2001) Geochemical study of seafloor hydrothermal system and chemosynthetic animal community around a submarine caldera, southern part of Kagoshima Bay, southern Kyushu, Japan. *JAMSTEC Deep-sea Res.*, **19**, 9–13 (in Japanese with English abstract).

(Editorial handling Takeshi Nishimura)

## 若尊カルデラ底の海底噴気孔の極近傍に設置した海底地震計で観測された 半日周潮的な周期性

八木原 寛・平野舟一郎・宮町宏樹・高山鐵朗・山崎友也・為栗 健・井口正人

桜島火山の北東に位置する若尊カルデラの海底において、海底地震計 (OBS) で観測された地動速度の振幅変化に、明瞭で半日周潮的な周期性が認められた。OBS の投入直後に、海底噴気孔から海面に浮上する気泡を視認したため、OBS で観測された地動はカルデラ底の海底噴気孔の活動によって生じたと考えられる。1 分毎の地動速度 RMS 振幅値 (RMSA) を求め、その変化と起潮力の理論値の変化、及び潮位計による水位の観測値の変化とを比較して得られた特徴は次のとおりである。1) 2007 年 9 月を通じて、RMSA に明瞭で半日周潮的な周期性が認められた。ただし、時々、不明瞭な期間があった。2) RMSA の極大の時刻が、起潮力の極大の時刻と時間領域で一致する。3) RMSA のパワースペクトルに認められる 4 つのピークの周波数は、主要 4 分潮の周波数と同一である。4) 詳細にみると、RMSA 変化はのこぎり刃状を呈する。また、日潮不等の期間においては、RMSA 変化が不規則であった。5) RMSA の長周期、または不規則な変化は、日潮不等の期間において卓越する。地熱システムの循環の一部を形成する、深部からカルデラ底に向かって上昇する地熱流体の活動が、起潮力によって増加するのであろう。